KYBERNETIKA — VOLUME *62* (2026), NUMBER 1, PAGES 77–98

PRESCRIBED-TIME PINNING CONTROL FOR DELAYED MEMRISTIVE NEURAL NETWORKS VIA EVENT-TRIGGERED STRATEGY

Xiaowei Meng, Yanlin Zhu, Hua Zhang and Quanjun Wu

This paper investigates the issues of prescribed-time synchronization for memristive neural networks with time-varying delay by event-triggered pinning control. To conserve resources and enhance control efficiency, two event-based control schemes and the measurement error function are obtained. Then, using Lyapunov stability theory and inequality techniques, some sufficient conditions are obtained to ensure the prescribed time synchronization of the response system and the drive system. Furthermore, under the two event trigger conditions, a positive lower bound on the inter-event time is derived respectively to ensure that Zeno behavior can be excluded during the whole time span except the prescribed settling time. Finally, numerical simulations are provided to illustrate the effectiveness of the obtained theoretical results.

Keywords: prescribed-time synchronization, event-triggered control, pinning control, memristive neural networks, Zeno behavior

Classification: 93C10, 34D06, 34D20

1. INTRODUCTION

The memristor, as the fourth basic element describing the relationship between charge and magnetic flux, was first proposed by Professor Chua in 1971 [3] and experimentally verified for the first time in 2008 at H-P laboratories [12]. Memristors makes it possible to achieve synaptic plasticity, which is a great advance in human simulation technology Since the memristor is a kind of natural synapse that can more accurately simulate the human brain, the memristor is introduced into the neural network to generate the memristor neural network (MNN) [11]. In recent years, memristor neural networks have been widely used in pattern recognition [20], image processing [4], pattern classification [21] and other application fields.

As is well known, event triggered control technology is an emerging discrete control technology in recent years, which has attracted much attention. Compared with continuous control methods, discontinuous control technology such as intermittent control [24], impulsive control [19], sampled-data control [22], and event-based control [17], etc, can reduce the control burdens. Different from other discontinuous control techniques, event-triggered control can decide when to execute a certain control strategy to ensure

DOI: 10.14736/kyb-2026-1-0077

the proper operation and stability of the system. In recent years, the application of event triggering control to study the dynamic behavior of neural networks has attracted wide attention [5, 16, 17]. For example, Wang investigated the global stochastic exponential stability of MNN under multiple network attacks by designing a dynamic event-triggered controller [17]. When large-scale neural networks are involved, it is impractical to exert control on each neuron, so it makes sense to guarantee synchronization by adopting a pinning control scheme, in which the controller is only added to a fraction of the systems to save control costs. In the synchronization of neural networks, many effective pining control schemes are proposed [7, 25, 28]. For instance, Guo applied distributed pinning control to study global exponential synchronization of multiple memristor neural networks in the presence of external noise [7]. Therefore, it is feasible to realize the synchronization of MNN via event-triggered pining control.

Many practical systems require consensus or synchronization to be reached within a specific time period, making it crucial to analyze and construct controllers to achieve faster convergence. Therefore, finite-time convergence is proposed to increase the rate of convergence, and it can achieve synchronization in finite time. For example, Ai addressed the problem of global finite-time stabilization by dynamic state feedback for a class of stochastic nonlinear systems [1]. But in fact the time required to reach synchronization depends on initial conditions. In order to make up for the deficiency of finite time convergence, fixed time convergence is proposed, which has the advantages of fast convergence speed and strong anti-interference ability. For instance, Gong studied finite/fixed-time synchronization problems for coupled MNNs [6]. However, it relies on other system parameters and still cannot be arbitrarily set by the designer according to actual needs. In order to make the settling time not affected by the initial state and system parameters, the prescribed time (PT) convergence is proposed, which is also the focus of research in recent years. Besides, such a technique was successfully used to solve prescribed-time consensus problem for dynamical networks [10], multi-agent systems [8], and neural networks [23]. However, there are few results for prescribed-time synchronization of MNNs by applying event-based control so far.

Based on the above analysis, we can see that it is meaningful to realize the PT synchronization of MNN by event triggering control. The main contributions include the following.

1) An event-based pinning control is proposed for realizing the PT synchronization of drive-response MNNs. The control is only applied to a portion of nodes and is only updated when the designed trigger conditions are fulfilled. It therefore offers more flexibility and applicability than many existing works.

2) The Lyapunov–Krasovsky functional selected in this paper avoids the use of any positive definite matrix, thereby significantly reducing the computational complexity in high-dimensional systems and large-scale coupled systems.

3) Two event triggering conditions are proposed, one with relatively fewer triggering times can reduce communication resources, and the other can avoid continuous state communication information between the drive-response systems.

The remainder of this paper is listed as follows. Section 2 introduces the drive-response MNNs and preliminaries. Section 3 provides the results relating to predefined-time synchronization by applying event-triggered control. In Section 4, the numerical simulations are presented. Finally, conclusions are drawn in Section 5.

2. PRELIMINARIES

Throughout this paper, the following notations will be used.

$\mathbb{R} = (-\infty, +\infty)$ denotes the set of real numbers, $\mathbb{R}_+ = (0, +\infty)$ denotes the set of nonnegative real numbers, $\mathbb{R}^n$ be the space of n-dimensional real column vectors and $\mathbb{R}^{n\times n}$ denotes the set of n×n real matrices, respectively. $\mathbb{V} = \{1, 2, \ldots, N\}$ be the set of positive integer numbers. The norms we use in this article are all 1-norm, i. e. for a vector $x = (x_1, x_2, \ldots, x_N)^\top$, $\|x\| = \sum_{i=1}^{N} |x_i|$, and for a matrix $A = [a_{ij}] \in \mathbb{R}^{N\times N}$, $\|A\| = \max_{1\le i\le N}\{\sum_{j=1}^{N} a_{ij}\}$. And sign(·) denotes the signum function.

2.1. System description

Consider the following drive MNNs with time-varying delays described as [13]

$$\dot{x_i}(t) = -d_i x_i(t) + \sum_{j=1}^{N} a_{ij}\big(x_i(t)\big) f_j\big(x_j(t)\big) + \sum_{j=1}^{N} b_{ij}(x_i(t)) f_j\big(x_j(t-\tau(t))\big),\ i \in \mathbb{V} \quad (1)$$

where $x_i(t)$ is the state variable of the ith neuron at time t; $d_i > 0$ is the self-inhibition of the ith neuron; $\tau(t)$ is transmission delay; $f_i(x_i(t))$ represents the neuron input–output activation of the ith neuron; $a_{ij}(x_i(t))$ and $b_{ij}(x_i(t))$ are the memristive feedback connection weight and the delayed feedback connection weight, for $i, j \in \mathbb{V}$. Based on the features of memristors, the memristive connection weights $a_{ij}(x_i(t))$ and $b_{ij}(x_i(t))$ satisfy the following conditions:

$$a_{ij}(x_i(t)) = \begin{cases} a_{ij}^{'}, & \text{if } |x_i(t)| \le k_i, \\ a_{ij}^{''}, & \text{if } |x_i(t)| > k_i, \end{cases}$$

$$b_{ij}(x_i(t)) = \begin{cases} b_{ij}^{'}, & \text{if } |x_i(t)| \le k_i, \\ b_{ij}^{''}, & \text{if } |x_i(t)| > k_i, \end{cases}$$

where k_i is the switching threshold, and $a_{ij}^{'}$, $a_{ij}^{''}$, $b_{ij}^{'}$ and $b_{ij}^{''}$ are all known constants. Throughout this paper, denote $\overline{a}_{ij} = \max\{|a_{ij}^{'}|, |a_{ij}^{''}|\}$, $\overline{b}_{ij} = \max\{|b_{ij}^{'}|, |b_{ij}^{''}|\}$, $\overline{A} = (\overline{a}_{ij})_{N\times N}$, and $\overline{B} = (\overline{b}_{ij})_{N\times N}$, for $i, j \in \mathbb{V}$.

Remark 2.1. As we all know, MNNs can be seen as a state-dependent switching system, The switching signal depends on state. If the memristive connection weights $a_{ij}(x_i(t))$ and $b_{ij}(x_i(t))$ keep fixed values, i. e. $a_{ij}^{'} = a_{ij}^{''}$, $b_{ij}^{'} = b_{ij}^{''}$ for $i, j \in \mathbb{V}$, then MNNs can be degraded into the version in [26].

The controlled response system of (1) can be described as follows

$$\dot{y_i}(t) = -d_i y_i(t) + \sum_{j=1}^{N} a_{ij}\big(y_i(t)\big) f_j\big(y_j(t)\big) + \sum_{j=1}^{N} b_{ij}(y_i(t)) f_j\big(y_j(t-\tau(t))\big) + u_i(t), \quad (2)$$

where $u_i(t)$, for $i, j \in \mathbb{V}$, is a controller designed for synchronization of the drive system (1) and response system (2).

Let the synchronization error $e_i(t) = y_i(t) - x_i(t)$, then the error system of systems (1) and (2) can be formulated as

$$\begin{aligned}\dot{e}_i(t) =& - d_i e_i(t) + \sum_{j=1}^{N} a_{ij}(y_i(t)) g_j\big(t\big) + \sum_{j=1}^{N} b_{ij}(y_i(t)) g_j\big(t - \tau(t)\big) \\ &+ \sum_{j=1}^{N} \big(a_{ij}(y_i(t)) - a_{ij}(x_i(t))\big) f_j(x_j(t) + \sum_{j=1}^{N} \big(b_{ij}(y_i(t)) - b_{ij}(x_i(t))\big) \\ &\times f_j\big(x_j(t - \tau(t))\big) + u_i(t),\end{aligned} \tag{3}$$

where $g_i(t) = f_i(y_i(t)) - f_i(x_i(t))$.

In addition, the error system (3) can be transformed into the following vector form

$$\begin{aligned}\dot{e}(t) =& - De(t) + A(y)g(t) + B(y)g\big(t - \tau(t)\big) + (A(y) - A(x))f\big(x(t)\big) \\ &+ (B(y) - B(x))f\big(x(t - \tau(t))\big) + U(t),\end{aligned} \tag{4}$$

where $e(t) = \big(e_1(t), \ldots, e_N(t)\big)^\top$, $D = \mathrm{diag}\big\{d_1, \ldots, d_N\big\}$, $f(t) = \big(f_1(t), \ldots, f_N(t)\big)^\top$, $A(x) = \big(a_{ij}(x_i(t))\big)_{n\times n}$, $A(y) = \big(a_{ij}(y_i(t))\big)_{n\times n}$, $B(x) = \big(b_{ij}(x_i(t))\big)_{n\times n}$, $B(y) = \big(b_{ij}(y_i(t))\big)_{n\times n}$, $U(t) = \big(u_1(t), \ldots, u_N(t)\big)^\top$, $g(t) = \big(g_1(t), \ldots, g_N(t)\big)^\top$.

Before moving on, a time-varying function in [2] is constructed as follows

$$w(t) = \begin{cases} \left(\dfrac{T}{T + t_0 - t}\right)^h, & \text{if } t \in [t_0, T_1), \\ 1, & \text{if } t \in [T_1, +\infty), \end{cases} \tag{5}$$

where $h > 2$ is a real number that can be given arbitrarily, $t_0 \geq 0$ is the initial time and T can be user-assignable, and $T_1 = t_0 + T$.

Due to the need for our results, necessary definition, assumption and useful lemmas are introduced below.

Definition 2.2. (Yang et al. [23]) For system (3), if the prescribed-time $T_1 = t_0 + T$ satisfies

$$\lim_{t\to T_1} e(t) = 0, \text{ and } e(t) = 0, \text{ for } t \in [T_1, +\infty), \tag{6}$$

then the prescribed-time synchronization is achieved, where T is the user-assignable time and T_1 is independent of initial states.

Definition 2.3. (Zhu and Jiang [29]) The system does not exhibit Zeno behavior if $\inf_k \big\{t_{k+1} - t_k\big\} > 0$, for all $k \in \mathbb{N}$, there is no trajectory of the system with an infinite number of events with a finite period of time.

Definition 2.4. (Zhou and Wu [27]) For a function $\mathcal{W}$: $\mathbb{R}^n \to \mathbb{R}_+$,

$$D^+\mathcal{W}(t) = \lim_{\varsigma \to 0^+} \sup \frac{1}{\varsigma}[\mathcal{W}(t+\varsigma) - \mathcal{W}(t)] \tag{7}$$

is called the upper right-hand Dini derivative of $\mathcal{W}$.

Assumption 2.5. (Wang et al. [18]) The activation function $f_i : \mathbb{R} \to \mathbb{R}$, is bounded, i. e. there exist constants $M_i > 0$ and $l_i > 0$, such that

$$|f_i(x)| \leq M_i, \ |f_i(x) - f_i(y)| \leq l_i|x-y|. \tag{8}$$

Remark 2.6. Assumption 2.5 is the Lipschitz condition. In practice, many practical models satisfy this assumption, such as Hopfield neural network, Chua circuit system, etc. Therefore, this paper assumes that Lipschitz condition is satisfied.

Assumption 2.7. (Liu et al. [9]) The time-varying delay $\tau(t)$ is differentiable and satisfies $0< \tau(t) < \tau$, $\dot{\tau}(t) \leq \rho < 1$.

Lemma 2.8. (Chen et al. [2]) If there exist a positive definite and continuously differentiable function V: $\mathbb{R}^n \to \mathbb{R}_+$, and positive constants $\beta_1 > 0$, $\beta_2 > 0$, $\frac{1}{h} - \beta_1 < \beta_3 < \frac{1}{h}$ such that

$$\begin{aligned} \dot{V}(t) &\leq -\beta_1 \frac{h}{T} w^{\frac{1}{h}}(t) V(t) + \beta_2 w^{\beta_3}(t), & t \in [t_0, T_1), \\ \dot{V}(t) &\leq -\beta_1 \frac{h}{T} w^{\frac{1}{h}}(t) V(t), & t \in [T_1, +\infty), \end{aligned}$$

where $T_1 = t_0 + T$, then the system (3) is said to be globally PT synchronization with the settling time T.

A sufficient condition for the prescribed-time stability was supplied in [18], which requires that $\dot{V}(t) \leq -bV(t) - 2\frac{\dot{w}(t)}{w(t)}V(t) \leq 0$ with $t \in [0, \infty)$ and $b > 0$. However, the result in Lemma 2.8 is different. It can be seen that $\dot{V}(t) > 0$ holds at some time belonging to $[t_0, T_1)$, which means that the condition in Lemma 2.8 is weaker and more applicable. Furthermore, when dealing with non-smooth systems or using non-smooth Lyapunov functions, the classical derivative tool may no longer be applicable. Hence, to ensure the universality and rigor of theoretical analysis, this paper will conduct a stability demonstration within the framework of Dini derivatives and the stability conclusion still holds [30].

2.2. The pinning control strategy relies on event-triggered mechanisms

Without loss of generality, let the nodes $i_1, i_2, \dots, i_m$ be selected as the pinned nodes, and the event-triggered pinning controller is designed as follows.

$$u_i(t) = \begin{cases} -\big(\alpha\frac{h}{T}w^{\frac{1}{h}}(t)+q_i\big)\Big[e_i(t_k)+\sigma(t_k)p_i\text{sign}(e_i(t_k))\Big]-\big(p_i \\ \quad +p_i\frac{h}{T}w^{\frac{1}{h}}(t)\big)\text{sign}\big(e_i(t_k)\big)-\alpha\frac{h}{T}w^{\frac{1}{h}}(t)\sum_{j=1}^{N}p_i\text{sign}\big(e_i(t_k)\big) \\ \quad \times\frac{\bar{b}_j}{1-\rho}\int_{t-\tau(t)}^{t}\big|g_j(s)\big)\big|\,\mathrm{d}s,\ i=1,2,\dots,m, \\ 0,\ \ i=m+1,m+2,\dots,N, \end{cases} \tag{9}$$

where $\sigma(t_k) = \sum_{j=m+1}^{N}|e_j(t_k)|$, $t \in [t_k, t_{k+1})$, $k \in \mathbb{N}$, t_k are triggering time instants, $\Delta(t_k) = t_{k+1} - t_k$ is called inter-event time, $\alpha > 0$, $q_i > 0$, θ and p_i will be determined later.

Remark 2.9. As mentioned in [25], pinning control can be applied to the synchronization of MNNs. In fact, coupling relationship also exists in MNNs whose state of each node can be influenced by other nodes. Such interaction implies that local disturbances or changes in a single node can propagate through the network, potentially leading to global behavioral changes. Therefore, by controlling only a subset of nodes and leveraging the coupling relationships between nodes, synchronization of the entire network can ultimately be achieved. Generally, increasing the number of controlled nodes results in faster convergence speed and enhanced synchronization performance of the network, as will be demonstrated in the subsequent numerical simulations.

To design an appropriate event-triggered control scheme, we define the measurement error as

$$\epsilon_i(t) = e_i(t_k) - e_i(t). \tag{10}$$

An event is triggered to update control when the measured error margin exceeds the state dependent threshold which is prescribed below.

3. MAIN RESULT

This section proposes the two appropriate event-triggered schemes, so that the response system (2) can be synchronized with the drive system (1) within predefined time.

3.1. The event-triggering condition is based on the error

Theorem 3.1. Suppose that Assumption 2.5 and 2.7 hold, PT synchronization for the drive system (1) and response system (2) can be achieved within the prescribed time T under the event-triggered condition as below

$$\|\epsilon(t)\| \le s(t) + \frac{\psi w^{-\frac{1}{h}}(t)\|e(t)\| + m\theta h}{\varphi}, \quad t \in [t_k, t_{k+1}), \tag{11}$$

where $\varphi = \kappa\alpha h + T\kappa q_{\max}$, $\psi = T(-\xi_{\max} l_{\max} + d_{\min} + \iota q_{\min})$, and the $s(t)$ is constructed as

$$s(t) = \begin{cases} w^{-b}(t), & \text{if } t \in [t_0, t_1), \\ 0, & \text{if } t \in [t_1, +\infty), \end{cases} \tag{12}$$

and $0 < b < \alpha\theta$, with the controller (9) satisfying

$$\iota q_{\min} \geq \max\{0,\, \xi_{\max} l_{\max} - d_{\min}\}, \tag{13}$$

$$\begin{cases} p_i > \gamma_i, & \text{if } \operatorname{sign}(e_i(t))\operatorname{sign}(e_i(t_k)) > 0, \\ p_i \leq -\gamma_i, & \text{if } \operatorname{sign}(e_i(t))\operatorname{sign}(e_i(t_k)) \leq 0, \end{cases} \tag{14}$$

where $\iota = \min\{1, m\theta\}$, $\kappa = \max\{1, m\theta\}$, $\xi_j = \sum_{i=1}^{N} \left(\bar{a}_{ij} + \frac{\bar{b}_j}{1-\rho}\right)$, $\bar{b}_j = \max_{1\leq i\leq N}\{\bar{b}_{ij}\}$, $\sum_{i=1}^{m} \gamma_i \geq \sum_{i=1}^{N} \left[\sum_{j=1}^{N} [|a'_{ij} - a''_{ij}| + |b'_{ij} - b''_{ij}|] M_j\right]$, $\theta = \min_{1\leq i\leq m}\{\gamma_i\}$, $\psi = -\xi_{\max} l_{\max} + d_{\min} + q_{\min}$.

Proof. Construct the following Lyapunov–Krasovsky functional candidate

$$V(t) = \sum_{i=1}^{N} |e_i(t)| + \sum_{i=1}^{N}\sum_{j=1}^{N} \frac{\bar{b}_j}{1-\rho} \int_{t-\tau(t)}^{t} \left|g_j(s)\right| \mathrm{d}s. \tag{15}$$

By calculating the upper right-hand derivative of $V(t)$ for $t \in [t_k, t_{k+1})$, and base on the definition of $b_{ij}(y_i)$ and $\bar{b}_{ij}$, we have

$$\begin{aligned} D^+V(t) \leq{}& \sum_{i=1}^{N} \operatorname{sign}(e_i(t)) \Bigg[-d_i e_i(t) + \sum_{j=1}^{N} a_{ij}(y_i(t)) g_j(t) + \sum_{j=1}^{N} b_{ij}(y_i(t)) \\ & \times g_j\big(t - \tau(t)\big) + \sum_{j=1}^{N} \big(a_{ij}\big(y_i(t)\big) - a_{ij}(x_i(t))\big) f_j\,(x_j(t)) + \sum_{j=1}^{N} \big(b_{ij}\big(y_i(t)\big) \\ & - b_{ij}(x_i(t))\big) f_j\big(x_j(t - \tau(t))\big) + u_i(t) \Bigg] + \sum_{i=1}^{N}\sum_{j=1}^{N} \frac{\bar{b}_j}{1-\rho} |g_j(t)| \\ & - \sum_{i=1}^{N}\sum_{j=1}^{N} \bar{b}_j \left|g_j\big(t - \tau(t)\big)\right| \\ \leq{}& \sum_{i=1}^{N} \operatorname{sign}(e_i(t)) \Bigg[-d_i e_i(t) + \sum_{j=1}^{N} a_{ij}\big(y_i(t)\big) g_j\big(t\big) + \sum_{j=1}^{N} \big(a_{ij}(y_i(t)) \\ & - a_{ij}(x_i(t))\big) f_j\big(x_j(t)\big) + \sum_{j=1}^{N} \big(b_{ij}(y_i(t)) - b_{ij}(x_i(t))\big) f_j\big(x_j(t - \tau(t))\big) \Bigg] \\ & - \sum_{i=1}^{m} \Bigg[\alpha\theta \frac{h}{T} w^{\frac{1}{h}}(t) e_i(t_k) - q_i e_i(t_k) - \alpha\theta \frac{h}{T} w^{\frac{1}{h}}(t) p_i \sigma(t_k) \operatorname{sign}(e_i(t_k)) - q_i p_i \end{aligned}$$

$$\times\,\sigma(t_k)\mathrm{sign}(e_i(t_k)) - \alpha\frac{h}{T}w^{\frac{1}{h}}(t)\sum_{j=1}^{N}p_i\mathrm{sign}(e_i(t_k))\frac{\bar{b}_j}{1-\rho}\int_{t-\tau(t)}^{t}|g_j(s))|\,\mathrm{d}s$$
$$- p_i\mathrm{sign}\big(e_i(t_k)\big) - p_i\frac{h}{T}w^{\frac{1}{h}}(t)\mathrm{sign}\big(e_i(t_k)\big)\Big] + \sum_{i=1}^{N}\sum_{j=1}^{N}\frac{\bar{b}_j}{1-\rho}\big|g_j(t)\big|. \tag{16}$$

It is obvious to obtain that

$$\begin{aligned}
&\sum_{i=1}^{N}\mathrm{sign}(e_i(t))\left[-d_ie_i(t) + \sum_{j=1}^{N}a_{ij}(y_i(t))g_j(t)\right] + \sum_{i=1}^{N}\sum_{j=1}^{N}\frac{\bar{b}_j}{1-\rho}\big|g_j(t)\big| \\
&\le\sum_{i=1}^{N}-d_i\big|e_i(t)\big| + \sum_{j=1}^{N}\sum_{i=1}^{N}\big(\bar{a}_{ij} + \frac{\bar{b}_j}{1-\rho}\big)\big|g_j(t)\big| \\
&\le\sum_{i=1}^{N}-d_i\big|e_i(t)\big| + \sum_{j=1}^{N}\xi_jl_j|e_j(t)| \\
&\le(-d_{\min} + \xi_{\max}l_{\max})\sum_{i=1}^{N}\big|e_i(t)\big|.
\end{aligned} \tag{17}$$

Based on the definition of measurement error $\epsilon_i(t)$, one can deduce

$$\begin{aligned}
&\sum_{i=1}^{m}\mathrm{sign}(e_i(t))\Big[-(\alpha\frac{h}{T}w^{\frac{1}{h}}(t)+q_i)e_i(t_k) - \alpha\frac{h}{T}w^{\frac{1}{h}}(t)\sum_{j=1}^{N}p_i\mathrm{sign}\big(e_i(t_k)\big)\frac{\bar{b}_{ij}}{1-\rho} \\
&\quad\int_{t-\tau(t)}^{t}\big|g_j(s)\big)\big|\,\mathrm{d}s - p_i(\alpha\frac{h}{T}w^{\frac{1}{h}}(t)+q_i)\mathrm{sign}(e_i(t_k))\sum_{j=m+1}^{N}|e_j(t_k)|\Big] \\
&\le-\alpha\frac{h}{T}w^{\frac{1}{h}}(t)\sum_{i=1}^{m}|e_i(t)| - m\theta\alpha\frac{h}{T}w^{\frac{1}{h}}(t)\sum_{j=1}^{N}\frac{\bar{b}_j}{1-\rho}\int_{t-\tau(t)}^{t}\big|g_j(s)\big)\big|\,\mathrm{d}s \\
&\quad - q_{\min}\sum_{i=1}^{m}|e_i(t)| + \big(\alpha\frac{h}{T}w^{\frac{1}{h}}(t)+q_{\max}\big)\sum_{i=1}^{m}|\epsilon_i(t)| - m\theta(\alpha\frac{h}{T}w^{\frac{1}{h}}(t) \\
&\quad + q_{\min})\sum_{j=m+1}^{N}|e_j(t)| + m\theta(\alpha\frac{h}{T}w^{\frac{1}{h}}(t)+q_{\max})\sum_{j=m+1}^{N}|\epsilon_j(t)| \\
&\le-\iota\alpha\frac{h}{T}w^{\frac{1}{h}}(t)\sum_{i=1}^{m}|e_i(t)| - \iota q_{\min}\sum_{i=1}^{N}|e_i(t)| - \frac{m}{N}\theta\alpha\frac{h}{T}w^{\frac{1}{h}}(t)\sum_{i=1}^{N}\sum_{j=1}^{N}\frac{\bar{b}_j}{1-\rho} \\
&\quad\times\int_{t-\tau(t)}^{t}\big|g_j(s)\big)\big|\,\mathrm{d}s + \kappa(\alpha\frac{h}{T}w^{\frac{1}{h}}(t)+q_{\max})\sum_{j=m+1}^{N}|\epsilon_j(t)| \\
&\le\nu\alpha\frac{h}{T}w^{\frac{1}{h}}(t)V(t) - \iota q_{\min}\sum_{i=1}^{N}|e_i(t)| + \kappa(\alpha\frac{h}{T}w^{\frac{1}{h}}(t)+q_{\max})\sum_{j=m+1}^{N}|\epsilon_j(t)|,
\end{aligned} \tag{18}$$

where $\iota = \min\{1, m\theta\}$, $\kappa = \max\{1, m\theta\}$, $\nu = \min\{1, \frac{m\theta}{N}\}$.
Based on (14), it is easy to prove that

$$\begin{aligned}
&-\sum_{i=1}^{m}(p_i + p_i\frac{h}{T}w^{\frac{1}{h}}(t))\mathrm{sign}(e_i(t))\mathrm{sign}(e_i(t_k)) + \sum_{i=1}^{N}\Bigg[\sum_{j=1}^{N}(a_{ij}(y_i(t)) - a_{ij}(x_i(t)))\\
&\quad\times f_j(x_j(t)) + \sum_{j=1}^{N}\big(b_{ij}(y_i(t)) - b_{ij}(x_i(t))\big)f_j\big(x_j(t-\tau(t))\big)\Bigg]\\
&\leq -\sum_{i=1}^{m}\gamma_i + \sum_{i=1}^{N}\left[\sum_{j=1}^{N}[|a_{ij}^{'} - a_{ij}^{''}| + |b_{ij}^{'} - b_{ij}^{''}|]M_j\right] - \sum_{i=1}^{m}\gamma_i\frac{h}{T}w^{\frac{1}{h}}(t)\\
&\leq -m\theta\frac{h}{T}w^{\frac{1}{h}}(t).
\end{aligned} \tag{19}$$

According to the event-triggered condition (11) and the fact that $w^{\frac{1}{h}}(t) \in [1, +\infty)$, one can deduce

$$\begin{aligned}
D^{+}V(t) \leq &(-d_{\min} + \xi_{\max}l_{\max} - \iota q_{\min})\sum_{i=1}^{N}|e_i(t)| - \nu\alpha\frac{h}{T}w^{\frac{1}{h}}(t)V(t)\\
&+ \kappa\big(\alpha\frac{h}{T} + q_{\max}\big)w^{\frac{1}{h}}(t)\sum_{i=1}^{N}|\epsilon_i(t)| - m\theta\frac{h}{T}w^{\frac{1}{h}}(t)\\
\leq &-\frac{\nu\alpha h}{T}w^{\frac{1}{h}}(t)V(t) + \kappa\big(\frac{\alpha h}{T} + q_{\max}\big)w^{\frac{1}{h}}(t)s(t).
\end{aligned} \tag{20}$$

In view of (12), one has

$$\begin{aligned}
&D^{+}V(t) \leq -\beta_1\frac{h}{T}w^{\frac{1}{h}}(t)V(t) + \beta_2 w^{\beta_3}(t), \quad t \in [t_0, T_1),\\
&D^{+}V(t) \leq -\beta_1\frac{h}{T}w^{\frac{1}{h}}(t)V(t), \qquad\qquad t \in [T_1, +\infty),
\end{aligned} \tag{21}$$

where $\beta_1 = \nu\alpha > 0$, $\beta_2 = \kappa(\frac{\alpha\theta h}{T} + q_{\max}) > 0$, $\beta_3 = \frac{1}{h} - b$.

As $0 < b < \alpha\theta$, it guarantees that $\frac{1}{h} - \beta_1 < \frac{1}{h} - b < \frac{1}{h}$. Therefore, we can conclude that the systems (1) and (2) can achieve PT synchronization referring to the results presented in Lemma 2.8. The proof is finished. □

Remark 3.2. Compared with the continuous controller reported in [15], the cumulative error $e_i(t_k)$ in controller (9) is only updated when the triggering condition (11) is fulfilled, requiring less computational burden when determining the control signal. It should be pointed out that, the continuous communication between drive system and response system is still required in order to compute the error item $|e(t)|$ in the trigger function (11).

Considering the constant time delay, i.e. $\tau(t) = \tau$, $\rho = 0$, we get the following Corollary 3.3.

Corollary 3.3. Suppose that Assumption 2.5 holds, PT synchronization of the drive system (1) and response system (2) can be achieved within the prescribed finite time T under the event-triggered condition as below

$$\|\epsilon(t)\| \leq s(t) + \frac{\psi w^{-\frac{1}{h}}(t)\|e(t)\| + \theta h}{\varphi}, \quad t \in [t_k, t_{k+1}), \tag{22}$$

where $\varphi = \kappa\alpha h + T\kappa q_{\max}$, $\psi = T(-\xi_{\max} l_{\max} + d_{\min} + \iota q_{\min})$, $\xi_j = \sum_{i=1}^{N}(\overline{a}_{ij} + \overline{b}_{ij})$.

Zeno behavior, a phenomenon of infinite number of samplings in a finite period of time, needs to be avoided when applying event-triggered control. Next, we ensure that Zeno behavior can be excluded during the control process by showing the existence of a positive lower bound of inter-event time.

Theorem 3.4. Given the protocol (9) with triggering condition (11), the system (3) has no Zeno behavior for $[\,0, T^{'}]$ and $[\,T^{''}, +\infty)$, where $T^{'}$ and $T^{''}$ are arbitrary values satisfying $T^{'} < T_1 < T^{''}$.

Proof. According to the proof of Lemma 2.8, we have

$$V(t) \leq (V(0) + \chi) w^{\beta_3 - \frac{1}{h}}(t), \tag{23}$$

where $\chi = \frac{\beta_2 T}{h(\beta_1+\beta_3)-1} > 0$.

Based on (15) and $w^{-b}(t) \in (0, 1]$, one has

$$\|e(t)\| = V(t) - \sum_{i=1}^{N}\sum_{j=1}^{N} \frac{\overline{b}_{ij}}{1-\rho} \int_{t-\tau(t)}^{t} |g_j(s)|\,\mathrm{d}s \leq V(0) + \chi. \tag{24}$$

We can get $\sigma(t_k) \leq \|e(t_k)\| \leq (V(0) + \chi)$. For $t \in [t_k, t_{k+1}) \in [t_0, T^{'})$, consider the derivative of $\|\epsilon(t)\|$

$$\begin{aligned}
D^{+}\|\epsilon(t)\| \leq & \|\dot{\epsilon}(t)\| = \|\dot{e}(t)\| \\
= & \big\| - De(t) + A(y) f\big(y(t)\big) - A(x) f\big(x(t)\big) + B(y) f\big(y(t-\tau(t))\big) \\
& - B(x) f\big(x(t-\tau(t))\big) - \alpha\frac{h}{T} w^{\frac{1}{h}}(t) e(t_k) - \alpha\frac{h}{T} w^{\frac{1}{h}}(t)\sigma(t_k) P \mathrm{sign}(e(t_k)) \\
& - Qe(t_k) - PQ\sigma(t_k)\mathrm{sign}(e(t_k)) - \alpha\frac{h}{T} w^{\frac{1}{h}}(t) P \mathrm{sign}\big(e(t_k)\big)\frac{\overline{B}}{1-\rho} \\
& \times \int_{t-\tau(t)}^{t} |g(s)|\,\mathrm{d}s - \big(P + P\frac{h}{T} w^{\frac{1}{h}}(t)\big)\mathrm{sign}(e(t_k))\big\| \\
\leq & \|D\|\|e(t)\| + 2\big(\|\overline{A}\| + \|\overline{B}\|\big)\|M\| + \big(\alpha\frac{h}{T} w^{\frac{1}{h}}(t) + \|Q\|\big)\|e(t_k)\| \\
& + \alpha\frac{h}{T} w^{\frac{1}{h}}(t) s\|P\| \frac{\|\overline{B}\|}{1-\rho} \int_{t-\tau(t)}^{t} \|g(s)\|\,\mathrm{d}s + \sum_{i=1}^{m} |p_i| + \frac{h}{T} w^{\frac{1}{h}}(t) \\
& \times \sum_{i=1}^{m} |p_i| + \sum_{i=1}^{m} p_i \alpha\frac{h}{T} w^{\frac{1}{h}}(t)\sigma(t_k) + \sum_{i=1}^{m} q_i p_i \sigma(t_k)
\end{aligned}$$

$$
\begin{aligned}
&\leq \|D\|\|\epsilon(t)\| + (\|D\| + \|Q\| + \alpha\frac{h}{T}w^{\frac{1}{h}}(t_{k+1})(V(0)+\chi) + 2\bigg[\|\overline{A}\| + \|\overline{B}\| \\
&\quad + \alpha\tau\frac{h}{T}w^{\frac{1}{h}}(t_{k+1})\|P\|\frac{\|\overline{B}\|}{1-\rho}\bigg]\|M\| + (1+\frac{h}{T}w^{\frac{1}{h}}(t_{k+1})\sum_{i=1}^{N}|p_i| \\
&\quad + (\sum_{i=1}^{m}p_i\alpha\frac{h}{T}w^{\frac{1}{h}}(t_{k+1}) + \sum_{i=1}^{m}q_ip_i)(V(0)+\chi) \\
&= \|D\|\|\epsilon(t)\| + \eta.
\end{aligned} \tag{25}
$$

where $M = (M_1, M_2 \ldots, M_N)^\top$, $Q = \mathrm{diag}\{q_1, q_2, \ldots, q_m, 0, \ldots, 0\}$, $P = \mathrm{diag}\{p_1, p_2, \ldots, p_m, 0, \ldots, 0\}$,$\overline{B} = (\bar{b}_1, \bar{b}_2, \ldots, \bar{b}_N)$, $\eta = (\|D\| + \|Q\| + \alpha\frac{h}{T}w^{\frac{1}{h}}(t_{k+1})(V(0)+\chi) + 2\bigg[\|\overline{A}\| + \|\overline{B}\| + \alpha\tau\frac{h}{T}w^{\frac{1}{h}}(t_{k+1})\|P\|\frac{\|\overline{B}\|}{1-\rho}\bigg] \times \|M\| + (1+\frac{h}{T}w^{\frac{1}{h}}(t_{k+1})\sum_{i=1}^{m}|p_i| + (\sum_{i=1}^{m}q_i\alpha\frac{h}{T}w^{\frac{1}{h}}(t_{k+1}) + \sum_{i=1}^{m}q_ip_i)(V(0)+\chi)$.

Due to $\|\epsilon(t_k)\| = 0$, then consider the following differential equation

$$
\begin{cases}
D^+\|\epsilon(t)\| = \|D\|\|\epsilon(t)\| + \eta, \\
\|\epsilon(t_k)\| = 0.
\end{cases}
$$

Hence, we have

$$
\|\epsilon(t)\| = \frac{\eta}{\|D\|}\left(e^{\|D\|(t-t_k)} - 1\right). \tag{26}
$$

According to comparison principle, (25) can be solved by

$$
\|\epsilon(t)\| \leq \frac{\eta}{\|D\|}\left(e^{\|D\|(t-t_k)} - 1\right). \tag{27}
$$

And the event triggered condition (11) implies that

$$
\|\epsilon(t_{k+1})\| \geq s(t) + \frac{\psi w^{-\frac{1}{h}}(t)\|e(t)\| + \theta h}{\varphi}. \tag{28}
$$

Based on (27) and (28), it is easy to prove that

$$
\Delta(t_k) \geq \frac{1}{\|D\|}\ln\left[1 + \frac{\|D\|s(t)}{\eta} + \frac{\|D\|\psi w^{-\frac{1}{h}}(t)}{\eta\varphi}\|e(t)\| + \frac{\|D\|\theta h}{\eta\varphi}\right]. \tag{29}
$$

When $t \in [0, T^{'}]$, since $s(t) \geq 0, |e_i(t)| \geq 0$, we have

$$
\Delta(t_k) > \frac{1}{\|D\|}\ln\left[1 + \frac{\|D\|\theta h}{\overline{\eta}\varphi}\right] > 0. \tag{30}
$$

where $\overline{\eta} = (\|D\| + \|Q\| + \alpha\theta\frac{h}{T}w^{\frac{1}{h}}(t_{k+1}))(V(0)+\chi) + 2\bigg[\|\overline{A}\| + \|\overline{B}\| + \alpha\tau\frac{h}{T}w^{\frac{1}{h}}(t_{k+1})\|P\| \times \frac{\|\overline{B}\|}{1-\rho}\bigg]\|M\| + (1+\frac{h}{T}w^{\frac{1}{h}}(t_{k+1}))\sum_{i=1}^{m}|p_i| + (\sum_{i=1}^{m}p_i\alpha\frac{h}{T}w^{\frac{1}{h}}(t_{k+1}) + \sum_{i=1}^{m}q_ip_i)(V(0)+\chi)$.

When $t \in [T^{''}, +\infty)$, one has

$$\Delta(t_k) > \frac{1}{\|D\|} \ln[1 + \frac{\|D\|\theta h}{\widetilde{\eta}\varphi}] > 0, \tag{31}$$

where $\widetilde{\eta} = (\|D\| + \|Q\| + \alpha\theta\frac{h}{T})(V(0) + \chi) + 2\left[\|\overline{A}\| + \|\overline{B}\| + \alpha\tau\frac{h}{T}\|P\|\frac{\|\overline{B}\|}{1-\rho}\right]\|M\| + (1 + \frac{h}{T})\sum_{i=1}^{N}|p_i| + (\sum_{i=1}^{m} p_i\alpha\frac{h}{T} + \sum_{i=1}^{m} q_i p_i)(V(0)+\chi)$. Therefore $\Delta(t_k) > \frac{1}{\|D\|}\ln[1+\frac{\|D\|\theta h}{\widetilde{\eta}\varphi}] > 0$. It thus completes the proof. □

Remark 3.5. It should be pointed out that, when $t \to T_1^-$, the function $w(t) \to \infty$, and Zeno behavior may occur at $t = T_1$. Moreover, there is no doubt that Zeno behavior, if it exists, must have occurred at some point fairly close to the settling time. This is reasonable because the control law should be updated at a higher frequency to achieve more precise control. In order to avoid $w(t)$ be quite large, one may select some T^* sufficiently close to T_1 subject to $T^* < T_1$, and set $w^{\frac{1}{h}}(T^*) = 0$. Thus the response system will approach certain small neighborhood of the drive system and remain unchanged. Similar to articles [10], this technique suffices to avoid the Zeno phenomenon at T_1, manifesting the applicability of our design in practice.

3.2. The event-triggering condition is not based on the error

In the following, we present a sufficient condition on synchronization with more conservative trigger function, which can avoid continuous state information.

Theorem 3.6. Suppose that Assumption 2.5 holds, the drive system (1) and response (2) can realize PT synchronization under the event-triggered condition as below

$$\frac{\eta}{\|D\|}(\exp(\|D\|(t - t_k)) - 1) - s(t) - \frac{\psi\mu(t) + m\theta h}{\varphi} \le 0, \tag{32}$$

where $t \in [t_k, t_{k+1})$, $\mu(t) = (V(0) + \chi)w^{\beta_3 - \frac{2}{h}}(t)$, q_i, p_i satisty (13) and (14), ψ, φ and θ are defined in Theorem 3.1.

Proof. Based on (15) and (23), one has

$$\begin{aligned}\sum_{i=1}^{N}|e_i(t)| &= V(t) - \sum_{i=1}^{N}\sum_{j=1}^{N}\frac{\overline{b}_{ij}}{1-\rho}\int_{t-\tau(t)}^{t}|g_j(s)|\,\mathrm{d}s \\ &\le (V(0) + \chi)w^{\beta_3 - \frac{1}{h}}(t).\end{aligned} \tag{33}$$

Under the event-triggered condition (32), and according to (27) and (20) one can deduce

$$\begin{aligned} D^+V(t) \leq &(-d_{\min} + \xi_{\max} l_{\max} - \iota q_{\min}) \sum_{i=1}^{N} |e_i(t)| - \frac{\nu\alpha h}{T} w^{\frac{1}{h}}(t) V(t) \\ &+ \kappa\big(\frac{\alpha h}{T} + q_{\max}\big) w^{\frac{1}{h}}(t) \sum_{i=1}^{N} |\epsilon_i(t)| - m\theta \frac{h}{T} w^{\frac{1}{h}}(t) \\ \leq &- \frac{\psi}{T}\big(V(0) + \chi\big) w^{\beta_3 - \frac{1}{h}}(t) - \nu\alpha \frac{h}{T} w^{\frac{1}{h}}(t) V(t) - m\theta \frac{h}{T} w^{\frac{1}{h}}(t) \\ &+ \kappa\big(\alpha \frac{h}{T} + q_{\max}\big) w^{\frac{1}{h}}(t) \frac{\eta}{\|D\|} \left(\exp\left(\|D\|(t - t_k)\right) - 1\right) \\ \leq &- \frac{\psi}{T}\big(V(0) + \chi\big) w^{\beta_3 - \frac{1}{h}}(t) - \alpha\theta \frac{h}{T} w^{\frac{1}{h}}(t) V(t) - m\theta \frac{h}{T} w^{\frac{1}{h}}(t) \\ &+ \kappa\big(\alpha\theta \frac{h}{T} + q_{\max}\big) w^{\frac{1}{h}}(t) s(t) \big(\alpha \frac{h}{T} + q_{\max}\big) w^{\frac{1}{h}}(t) \frac{\psi\mu(t) + m\theta h}{\varphi} \\ \leq &- \nu\alpha \frac{h}{T} w^{\frac{1}{h}}(t) V(t) + \kappa\big(\alpha\theta \frac{h}{T} + q_{\max}\big) w^{\frac{1}{h}}(t) s(t). \end{aligned} \tag{34}$$

Then, in view of the definition of $s(t)$ in (12), one has

$$\begin{aligned} D^+V(t) &\leq -\beta_1 \frac{h}{T} w^{\frac{1}{h}}(t) V(t) + \beta_2 w^{\beta_3}(t), \ t \in [t_0, T_1), \\ D^+V(t) &\leq -\beta_1 \frac{h}{T} w^{\frac{1}{h}}(t) V(t), \qquad\qquad\quad t \in [T_1, +\infty), \end{aligned} \tag{35}$$

where $\beta_1 = \nu\alpha > 0$, $\beta_2 = \kappa(\alpha\theta \frac{h}{T} + q_{\max}) > 0$, $\beta_3 = \frac{1}{h} - b$. Therefore, the PT synchronization can be achieved. The proof is completed. □

Considering the constant time delay, i. e. $\tau(t) = \tau$, $\rho = 0$, we get the following Corollary 3.7.

Corollary 3.7. Suppose that Assumption 1 holds, PT synchronization for the drive system (1) and response system (2) can be achieved within the prescribed finite time T under the event-triggered condition as below

$$\frac{\eta}{\|D\|} \left(\exp\left(\|D\|(t - t_k)\right) - 1\right) - s(t) - \frac{\psi\mu(t) + \theta h}{\varphi} \leq 0, \tag{36}$$

where $t \in [t_k, t_{k+1})$, $\varphi = \kappa\alpha\theta h + T\kappa q_{\max}$, $\psi = T(-\xi_{\max} l_{\max} + d_{\min} + \iota q_{\min})$, $\xi_j = \sum_{i=1}^{N} (\overline{a}_{ij} + \overline{b}_{ij})$.

As the similar proof of Theorem 3.4, the next result can be derived to avoid the Zeno behavior.

Theorem 3.8. The Zeno behavior can be excluded during the whole time span except the prescribed settling time T_1 in the case of Theorem 3.6.

P r o o f. By the definition of triggering time instants, when $t \in [t_k, t_{k+1})$ we have

$$\frac{\eta}{\|D\|}\left(\exp\left(\|D\|(t-t_k)\right)-1\right)-s(t)-\frac{\psi\mu(t)+\theta h}{\varphi}\geq 0. \tag{37}$$

One can derive that

$$\Delta(t_k)\geq\frac{1}{\|D\|}\ln\left[1+\frac{\|D\|(s(t)\varphi+\psi\mu(t)+\theta h)}{\eta\varphi}\right]. \tag{38}$$

Next, we prove that $\Delta(t_k)$ is uniformly bounded away from zero.

When $t \in [0, T^{'}]$, since s(t) ≥ 0, $\psi > 0$, $\eta^{'} \leq \overline{\eta}$, then it follows that

$$\frac{s(t)\varphi+\psi\mu(t)+\theta h}{\eta\varphi}>\frac{\psi\mu(t_k)+\theta h}{\overline{\eta}\varphi}>0. \tag{39}$$

Then

$$\Delta(t_k)\geq\frac{1}{\|D\|}\ln\left[1+\frac{\|D\|(\psi\mu(t_k)+\theta h)}{\overline{\eta}\varphi}\right]>0. \tag{40}$$

When $t \in [T^{''}, \infty]$, based on (12) and (5), one has

$$\Delta(t_k)\geq\frac{1}{\|D\|}\ln\left[1+\frac{\|D\|\left[\psi(V(0)+\chi)+\theta h\right]}{\widetilde{\eta}\varphi}\right]>0.$$

The proof is completed. □

Remark 3.9. By the triggering condition (32), it can be seen that the continuous state communication between drive system and response system is avoided to determine t_{k+1}. Compared with Theorem 3.1, the triggering conditions of Theorem 3.6 are more applicable, but the cost of the control scheme is relatively high due to the increase in triggering times, indicating that the triggering conditions of Theorem 3.1 and Theorem 3.6 have their own advantages and disadvantages in terms of applicability and reducing communication resources. This phenomenon will be further illustrated through the numerical simulations in the next section.

4. NUMERICAL SIMULATION

Example 4.1. Consider the 4-D MNNs described by:

$$\dot{x}_i(t)=-d_ix_i(t)+\sum_{j=1}^{4}a_{ij}(x_j(t))f_j(x_j(t))+\sum_{j=1}^{4}b_{ij}(x_j(t))f_j(x_j(t-\tau(t))),\ i\in\mathbb{V}, \tag{41}$$

where $\mathbb{V}=\{1,2,3,4\}$, $d_1=d_2=d_3=d_4=4$, $\tau_1(t)=\tau_2(t)=\tau_3(t)=\tau_4(t)=0.2$, which implies that $\rho=0$, and

$$A^{'}=\begin{bmatrix}-2.8 & 2.85 & -2.6 & 1.8\\ 1.75 & 2.9 & 0.36 & 2.6\\ -0.31 & -1.1 & 1.55 & -1.3\\ 2.6 & 1.2 & 1.8 & 2.65\end{bmatrix},$$

$$A'' = \begin{bmatrix} -2.9 & 2.85 & -2.5 & 1.9 \\ 1.75 & 2.8 & 0.31 & 2.6 \\ -0.36 & -1.3 & 1.55 & -1.3 \\ 2.6 & 1.21 & 1.8 & 2.65 \end{bmatrix},$$

$$B' = \begin{bmatrix} -0.11 & 0.38 & -0.55 & 0.93 \\ -0.6 & -0.08 & -1.2 & -0.9 \\ -0.5 & -1.6 & -1.5 & -1.7 \\ -0.8 & 1.7 & -1.5 & -1.5 \end{bmatrix},$$

$$B'' = \begin{bmatrix} -0.1 & -0.38 & -0.5 & 0.92 \\ -0.6 & -0.11 & -1.1 & -0.9 \\ -0.55 & -1.7 & -1.5 & -1.7 \\ -0.8 & 1.6 & -1.5 & -1.5 \end{bmatrix}. \tag{42}$$

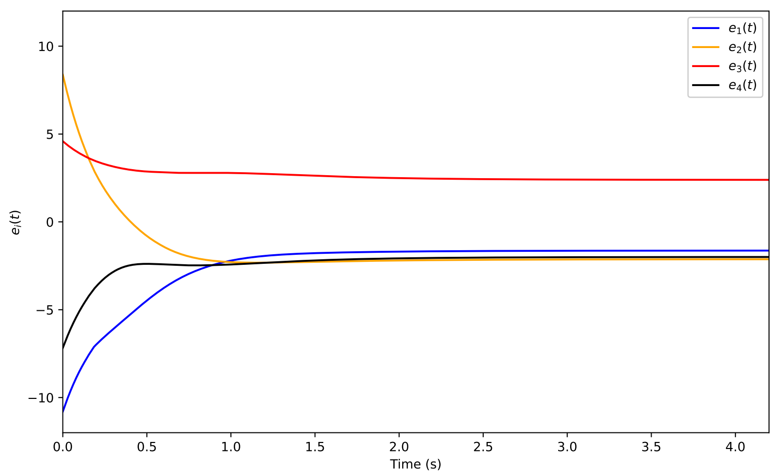

Fig. 1. The trajectories of $e_i(t)$ without control under $(x_1, x_2, x_3, x_4)^\top = (-4.26, 5.35, -2.32, 3.502)^\top$, $(y_1, y_2, y_3, y_4)^\top = (4.12, -5.45, 2.27, -3.675)^\top$.

Take the activation function $f_1(s) = f_2(s) = f_3(s) = f_4(s) = \tanh(s)$, Obviously, the activation function satisfying Assumption 1 with $l_1 = l_2 = l_3 = l_4 = 1, M_1 = M_2 = M_3 = M_4 = 1$.

The controlled response MNN is defined as:

$$\dot{y}_i(t) = -d_i y_i(t) + \sum_{j=1}^{4} a_{ij}(y_j(t)) f_j(y_j(t)) + \sum_{j=1}^{4} b_{ij}(y_j(t)) f_j\big(y_j(t-\tau(t))\big) + u_i(t), \tag{43}$$

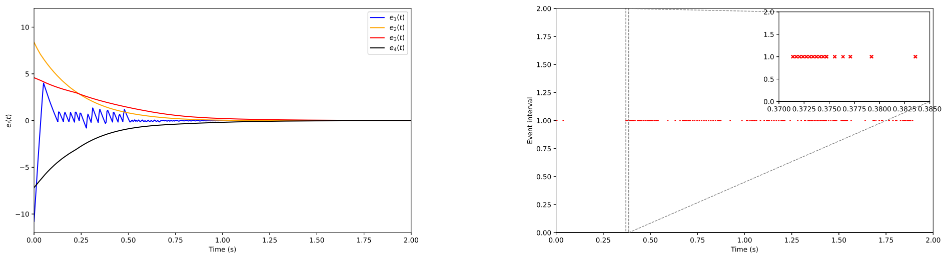

(a) (b)

Fig. 2. State error system trajectory and inter-event time under (44) by pinning a node chosen randomly with $(x_1, x_2, x_3, x_4)^\top = (-4.26, 5.35, -2.32, 3.502)^\top$, $(y_1, y_2, y_3, y_4)^\top = (4.12, -5.45, 2.27, -3.675)^\top$. (a) Synchronization error trajectory. (b) Triggering time instants.

where $u_1(t) = -\big(\alpha \frac{h}{T} w^{\frac{1}{h}}(t) + q_1\big)\Big[e_1(t_k) + \sigma(t_k)\text{sign}(e_1(t_k))\Big] - \big(p_1 + p_1 \frac{h}{T} w^{\frac{1}{h}}(t)\big)\text{sign}\big(e_1(t_k)\big) - \alpha \frac{h}{T} w^{\frac{1}{h}}(t) \sum_{j=1}^{N} p_2 \text{sign}\big(e_1(t_k)\big)\overline{b}_j \int_{t-\tau(t)}^{t} \big|g_j(s)\big|\,\text{d}s,\ t \in [t_k, t_{k+1})$, and $u_2(t) = u_3(t) = u_4(t) = 0$.

Based on the conditions in Corollary 3.3, we select $T = 3$, $t_0 = 0$, $\alpha = 2$, $h = 3$, $b = 0.2$, $q_1 = 11.75$. According to the definition of ξ_i, θ, γ_i, it is easy to obtain that $\xi_1 = 14.05$, $\xi_2 = 15.06$, $\xi_3 = 12.31$, $\xi_4 = 15.25$, $\gamma_2 \geq 1.16$. We choose γ_2=1.165, then $\theta = 1.165$, and let p_i satisfy

$$\begin{cases} p_1 = 1.2, & \text{if sign}(e_1(t))\text{sign}(e_1(t_k)) > 0, \\ p_1 = -1.2, & \text{if sign}(e_1(t))\text{sign}(e_1(t_k)) \leq 0. \end{cases}$$

Then we can derive the following event-triggered conditions

1) Event-triggering condition with error

$$\|\epsilon(t)\| \leq s(t) + 1/33 w^{-\frac{1}{h}}(t)\|e(t)\| + 4/55. \tag{44}$$

2) Event-triggering condition without error

$$\frac{\eta}{\|D\|}(\exp(\|D\|(t - t_k)) - 1) \leq s(t) + \mu(t)/33 + 4/55. \tag{45}$$

As shown in Figure 1, the drive system (41) and response system (43) cannot achieve synchronization without controller. It can be seen from Figure 2(a) and Figure 4(a), PT synchronization of the drive system (41) and response system (43) are achieved with controller within the theoretical synchronization time. Figure 2(b) and Figure 4(b) shows

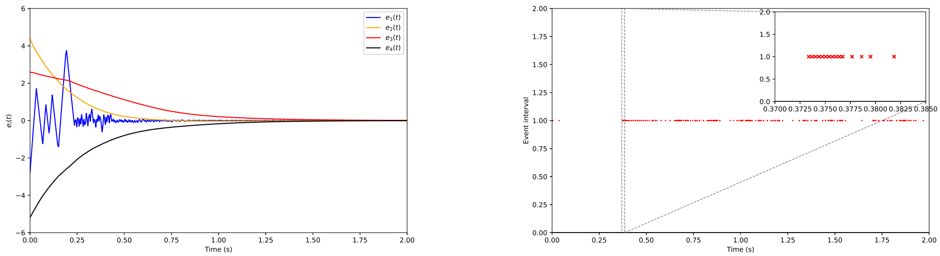

(a) (b)

Fig. 3. State error system trajectory and triggering time instants under (44) by pinning a node chosen randomly with $(x_1, x_2, x_3, x_4)^\top = (-2.26, 1.35, -1.32, 2.502)^\top$, $(y_1, y_2, y_3, y_4)^\top = (2.12, -1.45, 1.27, -2.675)^\top$. (a) Synchronization error trajectory. (b) Triggering time instants.

the accumulation of the triggering time instants is finite, which indicates that the Zeno behavior is excluded during the control process practically. We can also observe that the number of events triggered in Corollary 3.7 is significantly higher than in Corollary 3.3 in Figure 2(b) and Figure 4(b). The event triggering technique was proposed to reduce the control burden, indicating that the fewer the number of triggers within an appropriate range, the better. Based on the above analysis, both triggering conditions have their advantages and disadvantages. Although the triggering condition of Corollary 3.7 can avoid continuous state information between the driving system and response system, the number of triggering times is significantly increased.

In addition, if we change the initial value, i.e. $(x_1, x_2, x_3, x_4)^\top = (-2.26, 1.35, -1.32, 2.502)^\top$, $(y_1, y_2, y_3, y_4)^\top = (2.12, -1.45, 1.27, -2.675)^\top$, drive system and response system can still achieve synchronization at the PT, see Figure 3(a) and Figure 5(a). This further verifies that the initial condition do not affect the time when the drive-response MNNs achieve synchronization within a prescribed time. Figure 3(b) and Figure 5(b) also show that the Zeno behavior is excluded during the control process.

Furthermore, increasing the number of controlled nodes generally accelerates the convergence speed of the network. If we choose to control two nodes, one has $\gamma_1 + \gamma_2 \geq 1.16$. We choose γ_1=0.466, γ_1=0.7, then $\theta = 0.466$, and let p_i satisfy

$$\begin{cases} p_1 = 0.5, & \text{if } \mathrm{sign}(e_1(t))\mathrm{sign}(e_1(t_k)) > 0, \\ p_1 = -0.5, & \text{if } \mathrm{sign}(e_1(t))\mathrm{sign}(e_1(t_k)) \leq 0. \end{cases}$$

$$\begin{cases} p_2 = 0.75, & \text{if } \mathrm{sign}(e_1(t))\mathrm{sign}(e_1(t_k)) > 0, \\ p_2 = -0.75, & \text{if } \mathrm{sign}(e_1(t))\mathrm{sign}(e_1(t_k)) \leq 0. \end{cases}$$

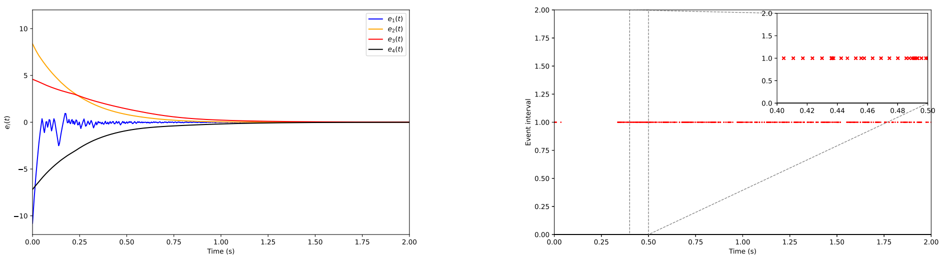

(a) (b)

Fig. 4. State error system trajectory and triggering time instants under (45) by pinning a node chosen randomly with $(x_1, x_2, x_3, x_4)^\top = (-4.26, 5.35, -2.32, 3.502)^\top$, $(y_1, y_2, y_3, y_4)^\top = (4.12, -5.45, 2.27, -3.675)^\top$. (a) Synchronization error trajectory of (41) and (43). (b) Triggering time instants.

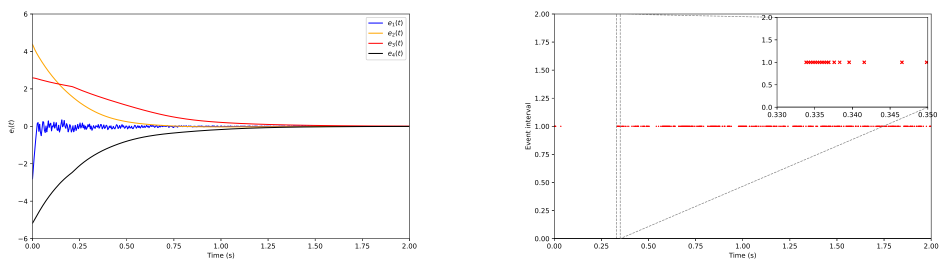

(a) (b)

Fig. 5. State error system trajectory and triggering time instants under (45) by pinning a node chosen randomly with $(x_1, x_2, x_3, x_4)^\top = (-2.26, 1.35, -1.32, 2.502)^\top$, $(y_1, y_2, y_3, y_4)^\top = (2.12, -1.45, 1.27, -2.675)^\top$. (a) Synchronization error trajectory. (b) Triggering time instants.

And event-triggering conditions are

$$\|\epsilon(t)\| \leq s(t) + 1/33w^{-\frac{1}{h}}(t)\|e(t)\| + 16/275, \tag{46}$$

and

$$\frac{\eta}{\|D\|}(\exp(\|D\|(t - t_k)) - 1) \leq s(t) + \mu(t)/33 + 16/275. \tag{47}$$

As shown in Figure 6(a) and Figure 6(b), the convergence speed of controlling two nodes is significantly faster than that of controlling one node. Furthermore, Figure 6(b) and Figure 6(d) also show that the Zeno behavior is excluded during the control process.

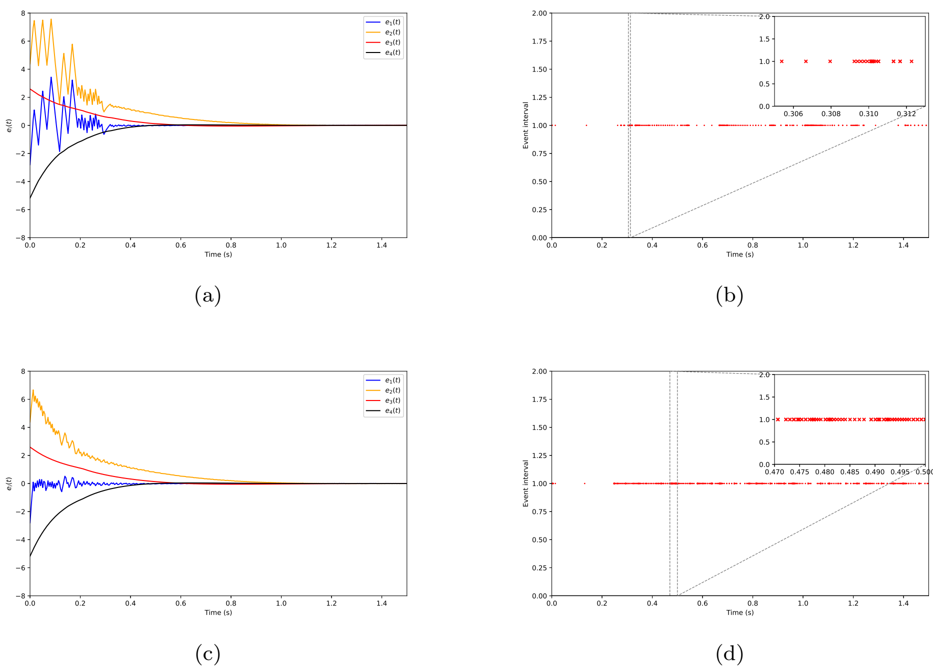

Fig. 6. State error system trajectory by pinning two nodes chosen randomly with $(x_1, x_2, x_3, x_4)^\top = (-2.26, 1.35, -1.32, 2.502)^\top$, $(y_1, y_2, y_3, y_4)^\top = (2.12, -1.45, 1.27, -2.675)^\top$. (a) State error system trajectory under (46). (b) Triggering time instants under (46). (c) State error system trajectory under (47). (d) Triggering time instants under (47).

5. CONCLUSION

In order to achieve the PT synchronization of the drive-response MNNs, a proper controller based on the event-triggered pinning control has been designed in this paper. Event triggering conditions with and without error have been proposed, and some sufficient conditions have been obtained based on these triggering conditions to achieve PT synchronization. Moreover, we have proved that the Zeno behavior is not exhibited during the entire time span except the settling time T_1. Finally, numerical simulation results have showed that event-triggered control strategy can reduce the burden of the network communication and the computational cost of the controller. In addition, we will consider the PT synchronization of MNN with uncertainties, limited communication bandwidth, and external stochastic disturbances via event trigger control in the future.

ACKNOWLEDGEMENT

This work was supported by key project of science and technology research program of Chongqing Education Commission of China (No.KJZD-K202401104).

(Received March 26, 2025)

REFERENCES

[1] W. Ai, J. Zhai, and S. Fei: Global finite-time stabilization for a class of stochastic nonlinear systems by dynamic state feedback. Kybernetika *49* (2013), 590–600. DOI:10.1007/s12035-013-8544-1

[2] X. Chen, H. Yu, and F. Hao: Prescribed-time event-triggered bipartite consensus of multiagent systems. IEEE Trans. Cybern. *52* (2022), 2589–2598. DOI:10.1109/TCYB.2020.3004572

[3] L. Chua: Memristor-the missing circuit element. IEEE Trans. Circuit Theory *18* (1971), 507–519. DOI:10.1109/TCT.1971.1083337

[4] M. Dong, S. Wen, Z. Zeng, Z. Yan, T. Huang: Sparse fully convolutional network for face labeling. Neurocomputing *331* (2019), 465–472. DOI:10.1016/j.neucom.2018.11.079

[5] Y. Fan, X. Huang, H. Shen, and J. Cao: Switching event-triggered control for global stabilization of delayed memristive neural networks: An exponential attenuation scheme. Neural Netw. *117* (2019), 216–224. DOI:10.1016/j.neunet.2019.05.014

[6] S. Gong, Z. Guo, S. Wen, and T. Huang: Finite-time and fixed-time synchronization of coupled memristive neural networks with time delay. IEEE Trans. Cybern. *51* (2021), 2944–2955. DOI:10.1109/TCYB.2019.2953236

[7] Z. Guo, S. Yang, and J. Wang: Global synchronization of memristive neural networks subject to random disturbances via distributed pinning control. Neural Netw. *84* (2016), 67–69. DOI:10.1016/j.jbankfin.2016.01.010

[8] X. Jia, H. Li, and X. Chi: Prescribed-time consensus of integrator-type multi-agent systems via sampled-data control. IEEE Trans. Circuits Syst. II Exp. Briefs *71* (2024), 3413–3417. DOI:10.1109/TCSII.2024.3361078

[9] H. Liu, J. A. Lu, J. Lu, and D. J. Hill: Structure identification of uncertain general complex dynamical networks with time delay. Automatica *45* (2009), 1799–1807. DOI:10.1016/j.automatica.2009.03.022

[10] D. Lyu, M. Sun, and Q. Jia: Event-based prescribed-time synchronization of directed dynamical networks with lipschitzian nodal dynamics. IEEE Trans. Circuits Syst. II Exp. Briefs *69* (2021), 1847–1851. DOI:10.1109/TCSII.2021.3134683

[11] Y. Pershin and M. D. Ventra: Experimental demonstration of associative memory with memristive neural networks. Neural Netw. *23* (2010), 881–886. DOI:10.1016/j.neunet.2010.05.001

[12] D. B. Strukov, G. S. Snider, D. R. Stewart, and R. S. Williams: The missing memristor found. Nature *453* (2008), 80–83. DOI:10.1038/nature06932

[13] H. Wang, S. Duan, T. Huang, and J. Tan: Synchronization of memristive delayed neural networks via hybrid impulsive control. Neurocomputing *267* (2017), 615–623. DOI:10.1016/j.neucom.2017.06.028

[14] K. Wang, Z. Teng, and H. Jiang: Adaptive synchronization of neural networks with time-varying delay and distributed delay. Physica A *387* (2008), 631–642. DOI:10.1016/j.physa.2007.09.016

[15] S. Wang and J. Jian: Predefined-time synchronization of fractional-order memristive competitive neural networks with time-varying delays. Chaos Solitons Fractals *174* (2023), 113790. DOI:10.1016/j.chaos.2023.113790

[16] Z. Peng, Z. Zhang, R. Luo, Y. Kuang, J. Hu, H. Cheng, and B. K. Ghosh: Event-triggered optimal control of completely unknown nonlinear systems via identifier-critic learning. Kybernetika *59* (2023), 365–391. DOI:10.14736/kyb-2023-3-0365

[17] X. Wang, J. H. Park, Z. Liu, and H. Yang: Dynamic event-triggered control for GSES of memristive neural networks under multiple cyber-attacks. IEEE Trans. Neural Netw. Learn. Syst. *35* (2024), 7602–7611. DOI:10.1109/TNNLS.2022.3217461

[18] Y. Wang, Y. Song, D. J. Hill, and M.Krstic: Prescribed-time consensus and containment control of networked multiagent systems. IEEE Trans. Cybern. *49* (2018), 1138–1147. DOI:10.1109/TCYB.2017.2788874

[19] Q. Wu, J. Zhou, and X. Lan: Impulses-induced exponential stability in recurrent delayed neural networks. Neurocomputing *74* (2011), 3204–3211. DOI:10.1016/j.neucom.2011.05.001

[20] W. Xu, S. Zhu, X. Fang, and W. Wang: Adaptive anti-synchronization of memristor-based complex-valued neural networks with time delays. Phys A *535* (2019), 122427. DOI:10.1016/j.physa.2019.122427

[21] Z. Yan, W. Liu, S. Wen, and Y. Yang: Multi-label image classification by feature attention network. IEEE Access *7* (2019), 98005–98013. DOI:10.1109/ACCESS.2019.2929512

[22] L. Yan, Z. Wang, Y. Zhang, and Y. Fan: Sampled-data control for mean-square exponential stabilization of memristive neural networks under deception attacks. Chaos Solitons Fractals *174* (2023), 113787. DOI:10.1016/j.chaos.2023.113787

[23] J. Yang, G. Chen, S. Zhu, S. Wen, and J. Hu: Fixed/prescribed-time synchronization of BAM memristive neural networks with time-varying delays via convex analysis. Neural Netw. *163* (2023), 53–63. DOI:10.1016/j.neunet.2023.03.031

[24] S. Yang, C. Li, and T. Huang: Exponential stabilization and synchronization for fuzzy model of memristive neural networks by periodically intermittent control. Neural Netw. *75* (2016), 162–172. DOI:10.1016/j.expthermflusci.2016.02.003

[25] Z. Yang, B. Luo, D. Liu, and Y. Li: Pinning synchronization of memristor-based neural networks with time-varying delays. Neural Netw. *93* (2017), 143–151. DOI:10.1016/j.neunet.2017.05.003

[26] H. Zhang, Z. Liu, G. B. Huang, and Z. Wang: Novel weighting-delay based stability criteria for recurrent neural networks with time-varying delay. IEEE Trans. Neur. Netw. *21* (2009), 91–106. DOI:10.1109/TNN.2009.2034742

[27] J. Zhou and Q. Wu: Exponential stability of impulsive delayed linear differential equations. IEEE Trans. Circuits Syst. II, Exp. Briefs *56* (2009), 744–48. DOI:10.1109/TCSII.2009.2027947

[28] J. Zhou, Q. Wu, and L. Xiang: Pinning complex delayed dynamical networks by a single impulsive controller. IEEE Trans. Circuits Syst. I Regul. Pap. *58* (2011), 2882–2893. DOI:10.1109/TCSI.2011.2161363

[29] W. Zhu and Z. P. Jiang: Event-based leader-following consensus of multi-agent systems with input time delay. IEEE Trans. Autom. Control *60* (2014), 1362–1367. DOI:10.1109/TAC.2014.2357131

[30] Y. Zhu and M. Jiang: Prescribed-time synchronization of inertial memristive neural networks with time-varying delays. AIMS Math. *10* (2025), 9900–9916. DOI:10.3934/math.2025453

Xiaowei Meng, School of Mathematics and Physics, Shanghai University of Electric Power, Shanghai, 201306, Shanghai. P. R. China.
e-mail: 18567410720@163.com

Yanlin Zhu, School of Mathematics and Physics, Shanghai University of Electric Power, Shanghai, 201306, Shanghai. P. R. China.
e-mail: zhuyanlin201@163.com

Hua Zhang, School of Science, Chongqing University of Technology, Chongqing, 400054, Chongqing. P. R. China.
e-mail: zhanghwua@163.com

Quanjun Wu, Corresponding author. School of Mathematics and Physics, Shanghai University of Electric Power, Shanghai, 201306, Shanghai. P. R. China.
e-mail: wuquanjun2008@163.com